Geophysical Research Letters

RESEARCH LETTER
10.1029/2023GL106964

Influence of Subsurface Critical Zone Structure on Hydrological Partitioning in Mountainous Headwater Catchments

Hang Chen[1], Qifei Niu[1], James P. McNamara[1], and Alejandro N. Flores[1]

[1]Department of Geosciences, Boise State University, Boise, ID, USA

Key Points:

- Integrated hydrologic modeling of catchments with different subsurface critical zone structures was performed
- Simulation results show that the shape of the weathered bedrock and associated storage capacity affect various hydrologic processes in the catchment
- The effect of weathered bedrock on hydrological partitioning is more significant under weather conditions featuring large snow fractions

Supporting Information:

Supporting Information may be found in the online version of this article.

Correspondence to:

Q. Niu,
qifeiniu@boisestate.edu

Citation:

Chen, H., Niu, Q., McNamara, J. P., & Flores, A. N. (2024). Influence of subsurface critical zone structure on hydrological partitioning in mountainous headwater catchments. *Geophysical Research Letters*, *51*, e2023GL106964. https://doi.org/10.1029/2023GL106964

Received 26 OCT 2023
Accepted 2 MAR 2024

Abstract Headwater catchments play a vital role in regional water supply and ecohydrology, and a quantitative understanding of the hydrological partitioning in these catchments is critically needed, particularly under a changing climate. Recent studies have highlighted the importance of subsurface critical zone (CZ) structure in modulating the partitioning of precipitation in mountainous catchments; however, few existing studies have explicitly taken into account the 3D subsurface CZ structure. In this study, we designed realistic synthetic catchment models based on seismic velocity-estimated 3D subsurface CZ structures. Integrated hydrologic modeling is then used to study the effects of the shape of the weathered bedrock and the associated storage capacity on various hydrologic fluxes and storages in mountainous headwater catchments. Numerical results show that the weathered bedrock affects not only the magnitude but also the peak time of both streamflow and subsurface dynamic storage.

Plain Language Summary In mountainous terrains, precipitation falling as snow and rain not only flows into streams but also infiltrates into the subsurface, replenishing the subsurface water storage. This stored water in the subsurface (including both soil moisture and rock moisture) supports various ecohydrological processes such as groundwater recharge and plant water use. In this study, we use computational simulation to study how the below-ground heterogeneity affects the partitioning of precipitation into streamflow, subsurface water storage, plant water use, and deep groundwater recharge. Here, below-ground heterogeneity refers to the depth extent of weathered rock at the hillslope- or catchment-scale. Simulation results show that both the annual magnitude and weekly variations of the streamflow and subsurface storage change noticeably as the below-ground weathering pattern varies, in particular under a snow-dominated weather scenario. The outcome of this study will potentially help stakeholders develop more informed water management practices in the face of a warming climate and more extreme weather events.

1. Introduction

Mountainous headwater catchments play a critical role in watershed functions (Evans et al., 2015). The headwater streams form the most extensive component of a stream network and provide significant amounts of water to higher-order streams (Welch & Allen, 2012). In addition, the groundwater flowing out of the headwater catchment can contribute to the larger parent watershed, particularly affecting the water quality and quantity in dry seasons (Ameli et al., 2018). To develop a predictive understanding of the streamflow in mountainous headwater catchments, we need to quantify how the precipitation is partitioned among various hydrologic processes and stages, including streamflow generation, plant water use, subsurface storage, and deep drainage recharging groundwater (Brooks et al., 2015; Roa-García et al., 2011). In the past several decades, many relevant works have been carried out using various methods, including field observations (Kormos et al., 2014), theoretical modeling (Bouaziz et al., 2018), and numerical simulations (Alatorre et al., 2012).

Recent studies have shown that hydrological partitioning could vary considerably across sites (e.g., Dralle et al., 2018; Wlostowski et al., 2021). By applying the Budyko framework, Wlostowski et al. (2021) found that many catchments in the Critical Zone Observatory (CZO) Network (Brantley et al., 2017) overproduce streamflow, and the departures below the theoretical Budyko curve may not be adequately explained by the fraction of precipitation falling as snow, as proposed in Berghuijs et al. (2014). The subsurface critical zone (CZ) structure has been invoked in their study to explain the observed overproduction of streamflow (Wlostowski et al., 2021). Similarly, other studies also used the subsurface CZ structure to explain various hydrologic observations in a number of catchments (e.g., Han et al., 2020; Klos et al., 2023; White et al., 2019). It is noted that

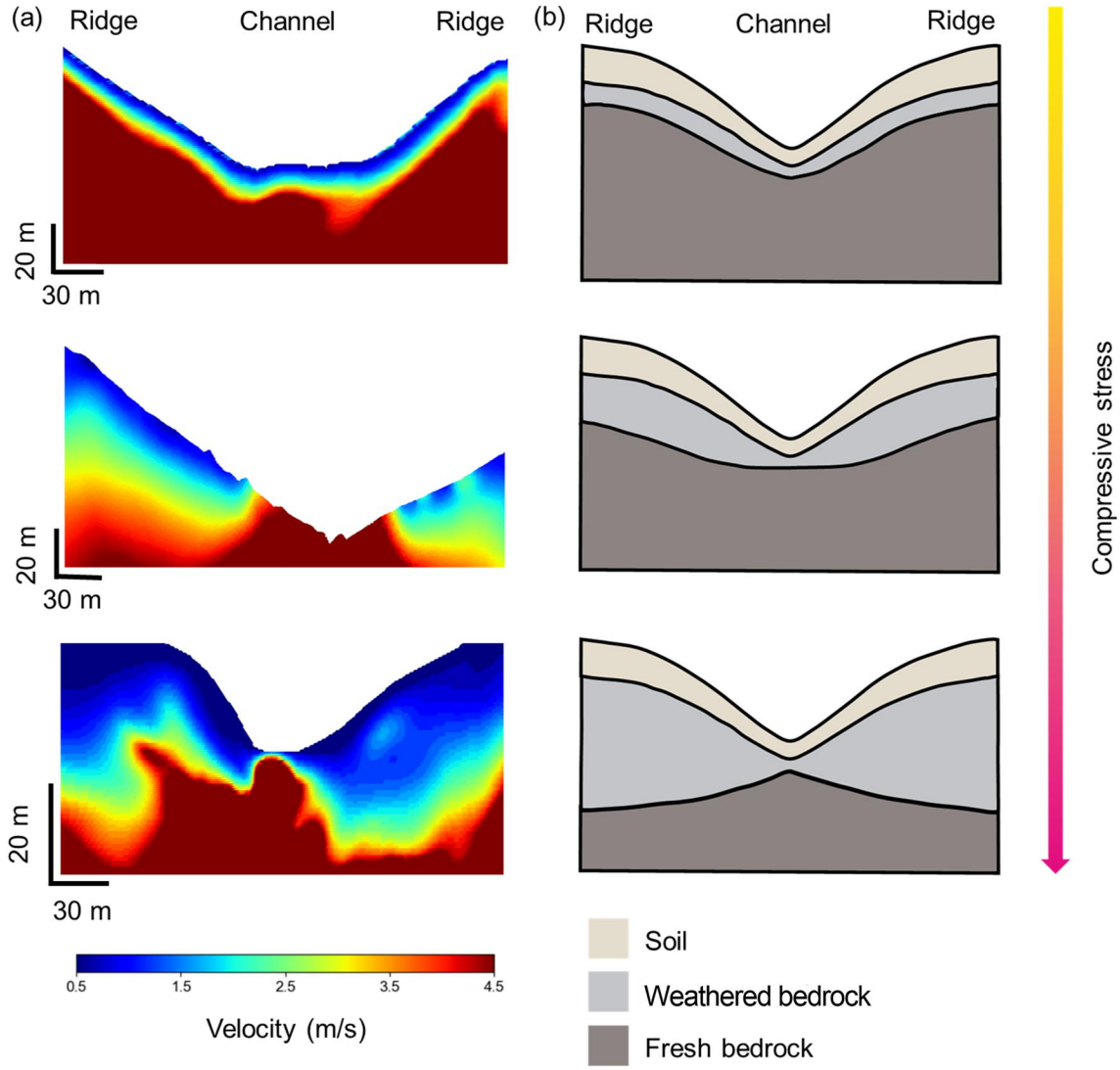

Figure 1. Subsurface critical zone structures of three sites in the United States (from top to bottom: Gordon Gulch, Colorado; Johnston Draw, Idaho; and Pond Branch, Maryland): (a) seismic P-wave velocity images and (b) the associated conceptual models. The seismic velocity data for Gordon Gulch and Pond Branch are from St Clair et al. (2015), and the data for Johnston Draw are from Nielson et al. (2021). Different shapes of the weathered bedrock and the associated storage capacity change were attributed to different horizontal compressive tectonic stresses relative to the vertical gravitational stresses (Riebe et al., 2017; St Clair et al., 2015).

aforementioned studies only have limited information on the subsurface CZ structure of the sites (i.e., the depth extent of structurally distinct layers such as soil and weathered rock), which are spatially heterogeneous in a catchment, even at the hillslope scale (e.g., Riebe et al., 2017). Traditional site characterization methods such as drilling and soil sampling may not work well to provide detailed spatial information on the subsurface CZ structure, hindering further understanding of the role of subsurface CZ structure in CZ hydrology.

Thanks to recent advances in geophysical imaging (Parsekian et al., 2015), the hillslope- or catchment-scale CZ structures have been revealed at some intensive study sites (e.g., St Clair et al., 2015). Figure 1 shows the 2D distributions of the seismic P-wave velocity at three sites in the United States (Nielson et al., 2021; St Clair et al., 2015) and the associated conceptual models of the subsurface CZ structure (Riebe et al., 2017) are also presented. In Figure 1, while the geometry of the soil layer is similar for the three sites, the weathered rock shows different geometries. At the Gordon Gulch in Boulder Creek CZO, Colorado (top panel in Figure 1), the weathered bedrock bottom is roughly parallel to the topographic surface ("parallel" type); at Pond Branch, Maryland (bottom panel in Figure 1), however, the weathered rock bottom mirrors the topographic surface ("mirror" type); the site at Johnston Draw in Reynolds Creek CZO, Idaho (middle panel in Figure 1) has an

intermediate feature. In addition to the shape, the volume of the weathered bedrock at each site is also different, giving different water storage capacities. Thus, in this study, the subsurface CZ structure mainly refers to both the shape of the weathered bedrock and the associated water storage capacity.

Different subsurface CZ structures shown in Figure 1 were attributed to different horizontal compressive tectonic stresses relative to the vertical gravitational stresses (St Clair et al., 2015). In general, when the ratio of horizontal tectonic stress over the gravitational stress is relatively large (bottom panel in Figure 1), the subsurface under the ridge will develop higher stresses and thus larger strains, which will promote weathering and forming a deeper weathered zone (Riebe et al., 2017; St Clair et al., 2015) if compared to the case when the ratio is low (top panel in Figure 1). More importantly, field observations have confirmed that catchments with different subsurface CZ structures could show different hydrologic functions (Wlostowski et al., 2021). For instance, the catchment sensitivity of runoff to storage changes in Gordon Gulch is ∼5 times higher than that in Johnston Draw (Wlostowski et al., 2021). Currently, it is unclear how the hillslope- or catchment-scale subsurface CZ structure (Figure 1) is linked to the water partitioning patterns and hydraulic functions in mountainous catchments.

The objective of this study is to explore how the subsurface CZ structure influences the hydrological partitioning in headwater catchments. In particular, we use a newly developed data-model fusion approach (Chen, Niu, Mendieta, et al., 2023) to study the effects of the shape of the weathered bedrock and associated storage capacity on the partitioning of precipitation in a hypothetical catchment, which is designed based on the 3D seismic velocity model (Chen, Niu, Mendieta, et al., 2023) of a headwater catchment in southern Idaho (the Dry Creek Experimental Watershed; see McNamara et al., 2018).

2. Models and Methods

2.1. Numerical Model

The headwater catchment in Chen, Niu, Mendieta, et al. (2023) is used here, and it occupies an area of approximately 0.02 km^2. The elevation of the catchment ranges between 1,590 and 1,650 m (Figure S1a in Supporting Information S1). The soil layer has a heterogamous thickness distribution (Figure S1b in Supporting Information S1), varying from 0 to 2.67 m and generally being thicker on ridges than valleys. Previous hydrologic modeling studies have been conducted at the site to study the streamflow generation (Kelleners et al., 2010) or bedrock drainage processes (Kormos et al., 2015). To study how subsurface CZ structure affects the hydrological partitioning, we designed three subsurface models (SM1-3) for the simulation. While the soil thickness distribution of the three models is identical, the spatial distribution of the weathered rock thickness is different for the three models (Figure S2 in Supporting Information S1). In model SM1, the bottom of the weathered bedrock generally parallels the ground surface, and the thickness ranges between 1.6 and 5 m with an average value of ∼2.6 m. Model SM3 (Figure S2c in Supporting Information S1) is similar to the case in the bottom panel of Figure 1, and its weathered rock bottom roughly mirrors the topographic surface; its thickness ranges from 0.3 to 45 m with an average value of ∼17 m. We also designed the model SM2, which has an intermediate thickness. These three synthetic models (SM1-3) represent typical subsurface CZ structures that are commonly observed in the field (e.g., Nielson et al., 2021).

2.2. Hydrologic Modeling

In this study, we employed the physically based hydrologic modeling code MODFLOW 6 (Bakker et al., 2016; Hughes et al., 2022) to simulate both surface and subsurface hydrologic processes and their interactions. In MODFLOW 6, the unsaturated-zone flow package is utilized to simulate vadose zone processes; the streamflow routing package is used to simulate stream flows; and the water mover package is used to track groundwater discharge and overland flow. The general-head boundary package is employed to account for head-dependent water flux leaving the model bottom, allowing for the simulation of deep drainage.

A snow model (SNOW-17, Anderson, 2006) was used to calculate the surface water input (SWI), which drives the integrated hydrologic modeling. In this study, the snow model parameters were taken from Chen, Niu, Mendieta, et al. (2023), which were calibrated using field-measured snow depth and density data. The potential evapotranspiration (ET) was estimated with the Penman-Monteith equation (Allen et al., 1998) using hydrometeorological data and a crop factor calibrated using MODIS data (Chen, Niu, Mendieta, et al., 2023).

In the simulations, each structural layer of the subsurface was treated as homogenous, and its hydrologic properties were calibrated using field measurements (Chen, Niu, Mendieta, et al., 2023). The variation ranges of these model parameters are summarized in Table S1 in Supporting Information S1. In this study, we performed a Monte Carlo simulation to estimate the uncertainty related to the simulated hydrologic fluxes and storages based on the variations in model parameters. Other model parameters were not calibrated, and their values were either taken from other studies or assigned based on experiences (Chen, Niu, Mendieta, et al., 2023). In the modeling, we followed the procedures in Maxwell and Kollet (2008) to run a spin-up phase, which forces the model to reach equilibrium by using the same hydrologic forcing repeatedly until the simulated hydraulic head change falls below a threshold.

2.3. Hydrometeorological Inputs

Hydrometeorological data are required to calculate SWI and potential ET. In this study, two weather conditions are considered. For the first weather scenario (W1), the field measured data in the water year 2013 (WC2013) at the catchment (McNamara et al., 2018) were used, including temperature (Figure S3a in Supporting Information S1), precipitation (Figure S3b in Supporting Information S1), solar radiation, humidity, etc. For this water year, the total precipitation is ∼688 mm, and snow accounts for ∼37.6% of the total precipitation, mostly falling from February to April. The measured streamflow is mostly during the snow season, totaling ∼145 mm. The temperature varies between −16°C and 29°C.

In addition to W1, we also designed a second weather condition (W2), which represents the snow-to-rainfall transition scenario. In many places in the western United States, the shifting from snow to rainfall has been observed (Dettinger et al., 2015). At the Dry Creek Experiment Watershed, the phase of precipitation has changed significantly in the last 10 years without apparent temperature change (McNamara et al., 2018). To simulate this snow-to-rain transition, we followed the method in Foster et al. (2016) to alter the temperatures during the snowfall to convert snow to rain. This adjustment in temperature during snowfall results in an elevated average temperature of only ∼0.47°C (Figure S3a in Supporting Information S1), but the precipitation is completely in the form of rain (Figure S3c in Supporting Information S1).

3. Results

In total, six simulations were conducted with three subsurface models (SM1, SM2, and SM3) and two weather scenarios (W1 and W2). The simulated hydrologic fluxes and storage are used to analyze how the subsurface CZ structure affects the partitioning of precipitation P into streamflow Q, deep drainage I, evaporation and plant water use ET_a, and subsurface water storage D. In particular, as the boundary between soil and weathered rock is explicitly defined in the subsurface models, both soil water storage and rock water storage can be quantified.

3.1. Annual Water Budget

Figure 2 shows the calculated water budget for all the simulations in WC2013, including Q, I, ET_a, soil dynamic storage D_s, and rock dynamic storage D_r. The dynamic soil (or rock) storage is calculated as the difference between the largest and smallest water storage in the soil (or weathered rock) during the water year, and it quantifies the amount of precipitation that actively contributes to the water dynamics in the soil (or weathered rock). Comparing the two weather scenarios (W1 and W2), no significant differences were observed for most of the water budget components (Figure 2). For instance, Q of subsurface model SM1 is ∼267 mm for W1 and ∼260 mm for W2. Considering this minor difference, discussions in this subsection are mainly based on the results of weather condition W1.

Among these hydrologic fluxes/storages, streamflow Q varies the most when subsurface CZ structures are changed (Figure 2). In general, as the weathered rock layer becomes thicker (from SM1 to SM3), Q decreases significantly by ∼122 mm for weather condition W1. This decreasing trend indicates that hillslope/catchment with the weathered rock bottom parallel to the ground surface promotes streamflow generation. This effect can be explained using the fill-and-spill concept (McDonnell et al., 2021), which states that only when the subsurface storage is added to reach a critical level does the outflow pathway become connected, resulting in significant streamflow. Subsurface with the weathered rock bottom mirroring the ground surface (e.g., SM3) clearly has a much larger storage capacity, and therefore, more precipitation is required to fill the storage deficit before generating significant streamflow (spill); the consequence is much smaller streamflow (reduced by ∼122 mm)

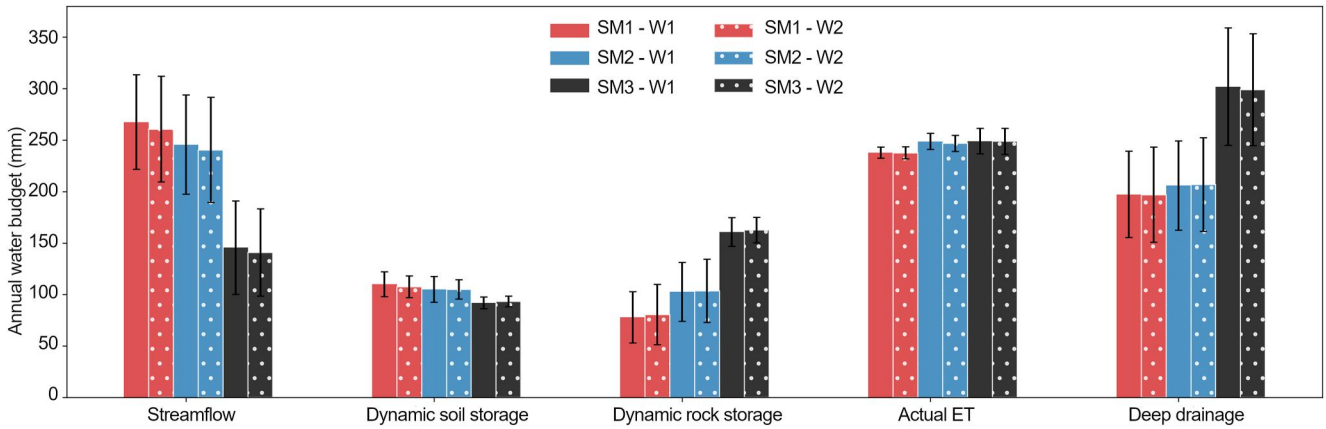

Figure 2. Simulated water budget components in the water year 2013 for different subsurface models (SM1, SM2, and SM3) with two weather conditions (W1 and W2). The uncertainty (error bar) is determined as the standard deviation of 500 random hydrologic simulation results.

and higher rock storage (increased by ~83 mm) as shown in Figure 2. This simulation result is also consistent with Wlostowski et al. (2021), which showed that dominant shallower subsurface flow may lead to overproduction of streamflow.

The influence of subsurface CZ structure on dynamic rock storage also has a cascading effect on other hydrologic fluxes, such as the deep drainage (i.e., water leaving the catchment through the lower boundary of the model). As shown in Figure 2, more deep drainage occurs in SM3 (~301 mm) than in SM1 (~197 mm). This trend can be explained by the increased rock storage in SM3, which promotes deep drainage by increasing the water level in the bedrock. The dynamic storage in the soil layer is similar (~100 mm) for all six simulations due to the thin soil thickness (less than 3 m; Figure S1b in Supporting Information S1). The actual ET (ET_a) of these six models is also similar (~250 mm) as there are no significant changes in the energy demand (e.g., air temperature; Figure S3 in Supporting Information S1). In addition, in the simulation, we limit plant water uptake to the top two meters (similar to the root depth of shrubs), and the available water (mainly in the soil layer) for ET did not change significantly among models (Figure 2).

3.2. Seasonal Water Dynamics

The simulated weekly water fluxes and storages with weather condition W1 are shown in Figure 3 for all the subsurface models (SM1, SM2, and SM3). The plotted parameters include SWI, Q, D_s, D_r, and I. The actual ET (ET_a) was not included in Figure 3 due to the insignificant differences observed among these subsurface models (Figure S4 in Supporting Information S1). The results in Figure 3 show some general features for all the models. First, during the snowmelt season from February to April, overland flow (Figure 3a), streamflow (Figure 3b), and soil storage (Figure 3c) are in phase (e.g., all are peaking in later February or early March), implying that the streamflow generation at this catchment is dominated by fast flow paths through the overland flow and/or interflow (Heidbüchel et al., 2012). Second, the soil water storage (Figure 3c) generally peaks earlier and faster than the rock water storage (Figure 3d), and the time for soil and rock to reach their lowest storage is also different (July vs. November). Lastly, the deep drainage rate appears constant throughout the year for all the models (Figure 3e), indicating the groundwater level variation is much smaller than the total head applied at the bottom of the models (Figure S5 in Supporting Information S1). This also implies that the deep drainage rates of the models here are primarily controlled by the low permeability of the fresh bedrock (Table S1 in Supporting Information S1).

Despite these common features, some differences are also observed for these three subsurface models. First, the streamflow produced in SM3 (Figure 3b) is systemically lower than that in SM1, and so is the soil water storage (Figure 3c); most of the differences occur during the snowmelt reason (i.e., from February to April). Since the ground surface and soil layer are identical for SM1 and SM3, the observed low Q and D_s in SM3 must result from the weathered bedrock. As shown in Figure 1b, SM3 generally has a larger volume of weathered rock (and thus water storage capacity) than SM1. This larger storage capacity potential in SM3 allows the catchment to store

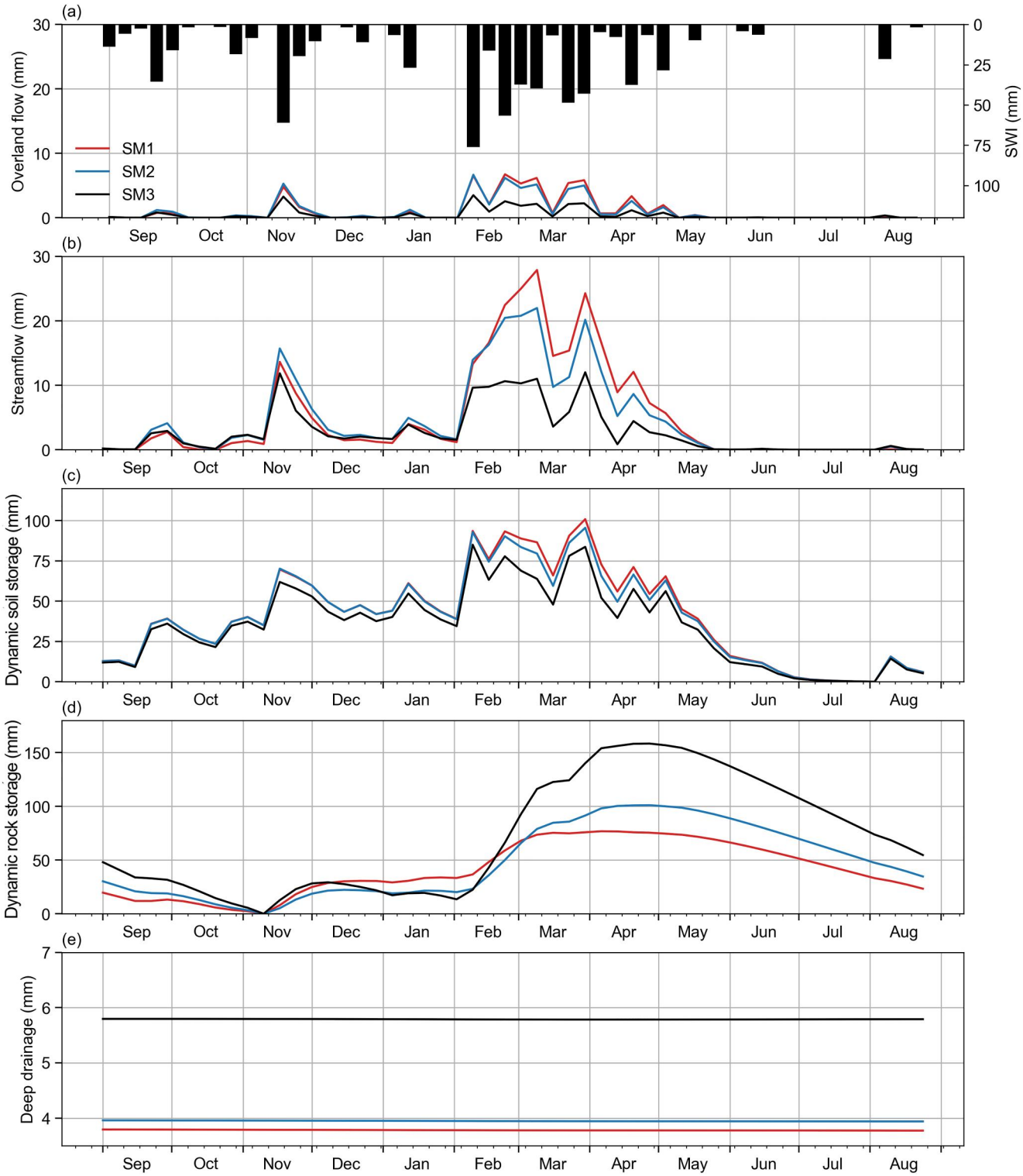

Figure 3. Simulated weekly water fluxes and storages of the catchment with different subsurface models (SM1, SM2, and SM3) under the weather condition W1: (a) surface water input and overland flow, (b) streamflow, (c) dynamic soil storage, (d) dynamic rock storage, and (e) deep drainage. The data in the figure are the average values of 500 random hydrologic simulation results.

much more water during the wet season (i.e., snowmelt), as shown in Figure 3d. For instance, the rock water storage at the end of April is ∼150 mm in SM3, but it is only ∼76 mm in SM1. Considering that the total precipitation, soil water storage, and ET_a are similar, larger water storage in the weathered rock means there will be less surface water generated (i.e., overland flow and streamflow), as shown in Figures 3a and 3b. The deep drainage at the bottom of the model is consistently larger in SM3 than in SM1, implying a higher water level in SM3, which is consistent with its high rock water storage (Figure 3d).

In addition to the magnitude, the time when the water fluxes/storages reach their maximum is also different for the three subsurface models. For instance, the peak streamflow time is around the first week of March in SM1, but it is at the end of March for SM3. For the rock water storage, the peak time is around late April for SM3, but it is in early March for SM1. The peak time differences can also be explained by the larger rock storage capacity associated with SM3. Compared to SM1, SM3 needs more surface water to replenish the rock storage deficiency, thus consuming more soil moisture in the early snowmelt season (late February and early March). This process will not only decrease the soil moisture (Figure 3c) but also reduce the interflow that would otherwise contribute to the streamflow (Figure 3b). As more time is required to replenish the larger rock storage in SM3, the time for the rock to reach its maximum storage is relatively later in SM3 than that in SM1, as shown in Figure 3d.

3.3. Comparison of Different Weather Conditions

Many studies have investigated the influence of precipitation patterns on the hydrological partitioning (e.g., Maxwell & Kollet, 2008; Wang et al., 2018). Numerous studies suggested that runoff efficiency in rain-dominated and snow-dominated catchments are different due to the lagged surface water input from snowmelt. As there is an observed snow-to-rainfall transition trend in the western United States (Dettinger et al., 2015), it is worthwhile to study if the observed effects of subsurface CZ structures still hold under the weather with 100% rainfall. We use the weekly water fluxes and storages calculated from the weather scenario W2 (Figure 4) to explore the answer to this question.

Similar to results in W1 (Figure 3), we also observed that the overland flow, dynamic soil storage, and streamflow are in general synchronized in Figure 4, highlighting the importance of short flow paths (overland flow and interflow) in the streamflow generation of this catchment. The delayed rock water storage responses and constant deep drainage rate are also observed in Figure 4. In addition, the effect of subsurface CZ structure on the magnitude of various water fluxes/stages is also obvious. For instance, streamflow (Figure 4b) is significantly lower in SM3 than in SM1; the rock water storage varies much smoother throughout the year (Figure 4d) and peaks at a much later time than the soil water storage. Again, these observed differences between SM1 and SM3 can be explained by the different rock storage capacities, as discussed in Section 3.2.

However, the peak time difference among the three subsurface models is not observed for the streamflow and rock water storage in Figure 4. As shown in the figure, peak streamflow time for all the subsurface models is the same, around the end of March; the rock water storage of the three models reach their peaks all in early April. This implies that the partitioning of rain is less influenced by the subsurface CZ structures if compared to precipitation with a large snow fraction (W1). If we take a close look at Figures 3a and 4a, it can be found that SWI under W2 showed less variability than W1. Less variability in Figure 4a means SWI provides a more stable water input to the subsurface during the wet season such that both soil and rock water storages can be quickly replenished, reaching their peak storages earlier than that under W1. For instance, all the models under W2 (Figure 4d) reach their highest rock storage in early April, but under W1 (Figure 3d), the rock storage keeps increasing until the end of April. Due to this consistent and fast replenishment in W2, no peak time differences were observed for rock water storage among different subsurface models, as shown in Figure 4.

4. Conclusion

The numerical simulation performed in this study revealed that the subsurface CZ structure has a significant influence on the partitioning of precipitation in mountainous headwater catchments. In general, catchments with a "mirror" type of weathered bedrock, probably due to high horizontal compressive tectonic stress, usually need more water from the soil layer to replenish its storage deficiency during wet seasons. Thus, compared to catchments with a "parallel" type of weathered bedrock, catchments with the "mirror" type of weathered bedrock tend to hinder streamflow generation. In addition, more water stored in the weathered bedrock will also promote deep drainage by increasing the groundwater level.

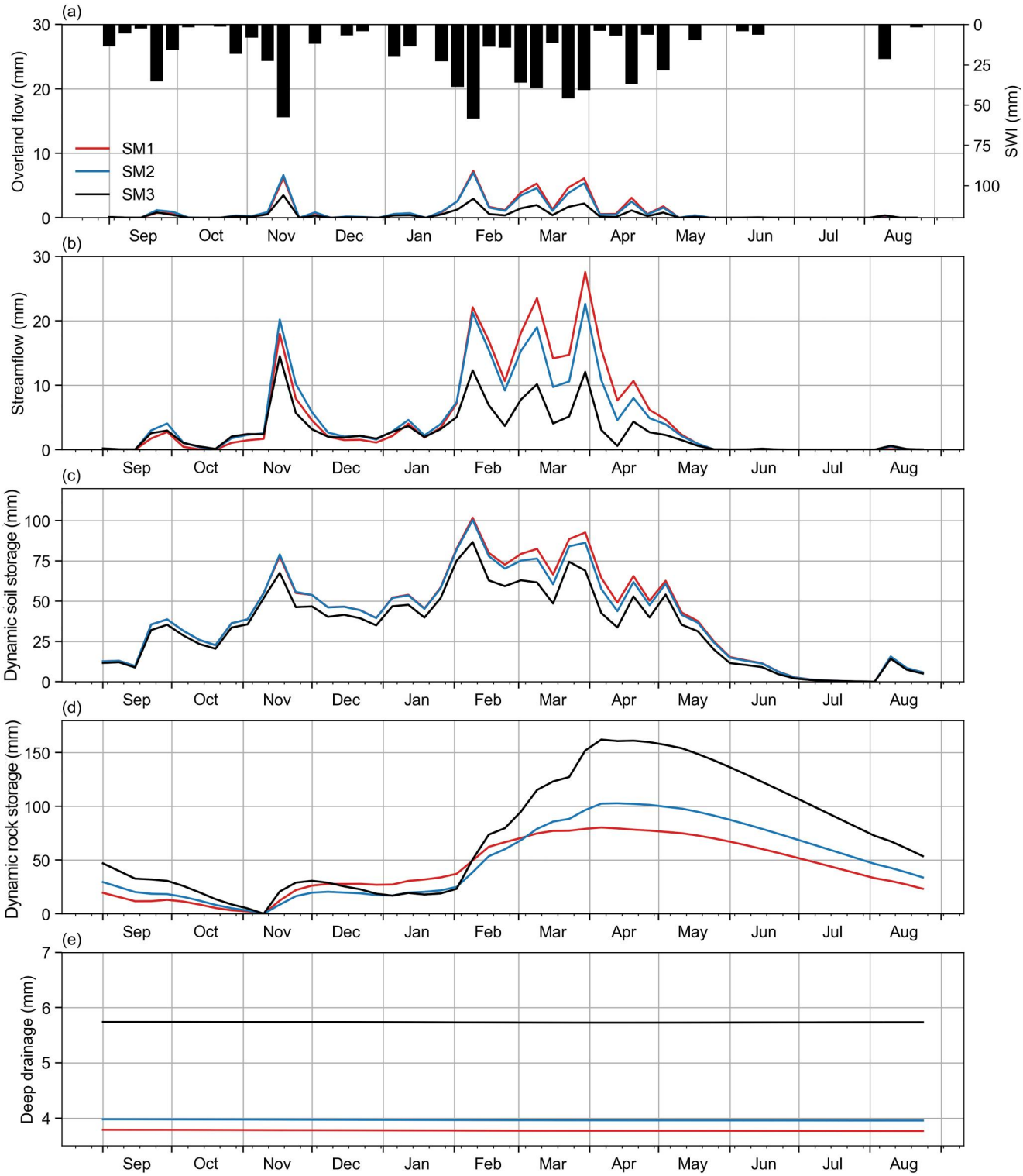

Figure 4. Simulated weekly water fluxes and storages of the catchment with different subsurface models (SM1, SM2, and SM3) under the weather condition W2: (a) surface water input and overland flow, (b) streamflow, (c) dynamic soil storage, (d) dynamic rock storage, and (e) deep drainage. The data in the figure are the average values of 500 random hydrologic simulation results.

Moreover, the subsurface CZ structure can also affect the time when the streamflow and dynamic soil/rock water storage reach their maximum. Under weather conditions with significant snowfalls, rapid snowmelt can quickly convert a significant amount of precipitation into streamflow, leaving less water to recharge subsurface storage. Due to its small storage capacity, a catchment with a "parallel" type of weathered bedrock will be fully recharged earlier than the catchment with a "mirroring" type of bedrock. In contrast, rainfall-dominated weather will replenish the subsurface storage more consistently than snow-dominated weather. With rainfall, catchments with different subsurface structures tend to be recharged relatively quickly, showing no obvious difference in the peak time. The findings of this study have significant implications for future water management strategies, particularly in regions where the precipitation has a high fraction of snow.

Data Availability Statement

The hydrometeorological data, numerical data, and MODFLOW model used in this study can be obtained from Chen, Niu, McNamara, and Flores (2023).

Acknowledgments
We would like to acknowledge the high-performance computing support of the Borah compute cluster (https://doi.org/10.18122/oit/3/boisestate) provided by Boise State University's Research Computing Department. HC would like to thank the support from the SEG Foundation/Chevron and the Gary and Lorene Servos Scholarship. We thank two anonymous reviewers for their invaluable comments, which have improved the quality of this manuscript. This study is partially supported by the National Science Foundation under grants EAR#2330004 and EAR#2054805.

References

Alatorre, L. C., Beguería, S., Lana-Renault, N., Navas, A., & García-Ruiz, J. M. (2012). Soil erosion and sediment delivery in a mountain catchment under scenarios of land use change using a spatially distributed numerical model. *Hydrology and Earth System Sciences*, *16*(5), 1321–1334. https://doi.org/10.5194/hess-16-1321-2012

Allen, R. G., Pereira, L. S., Raes, D., & Smith, M. (1998). Crop evapotranspiration-guidelines for computing crop water requirements-FAO irrigation and drainage paper 56. *Fao, Rome*, *300*(9), D05109.

Ameli, A. A., Gabrielli, C., Morgenstern, U., & McDonnell, J. J. (2018). Groundwater subsidy from headwaters to their parent water watershed: A combined field-modeling approach. *Water Resources Research*, *54*(7), 5110–5125. https://doi.org/10.1029/2017wr022356

Anderson, E. A. (2006). *Snow accumulation and ablation model: NWSRFS (National weather service river forecast system) Snow17 snow model* (Vol. 81). User Manual for Release.

Bakker, M., Post, V., Langevin, C. D., Hughes, J. D., White, J. T., Starn, J. J., & Fienen, M. N. (2016). Scripting MODFLOW model development using Python and FloPy. *Ground Water*, *54*(5), 733–739. https://doi.org/10.1111/gwat.12413

Berghuijs, W. R., Woods, R. A., & Hrachowitz, M. (2014). A precipitation shift from snow towards rain leads to a decrease in streamflow. *Nature Climate Change*, *4*(7), 583–586. https://doi.org/10.1038/nclimate2246

Bouaziz, L., Weerts, A., Schellekens, J., Sprokkereef, E., Stam, J., Savenije, H., & Hrachowitz, M. (2018). Redressing the balance: Quantifying net intercatchment groundwater flows. *Hydrology and Earth System Sciences*, *22*(12), 6415–6434. https://doi.org/10.5194/hess-22-6415-2018

Brantley, S. L., McDowell, W. H., Dietrich, W. E., White, T. S., Kumar, P., Anderson, S. P., et al. (2017). Designing a network of critical zone observatories to explore the living skin of the terrestrial Earth. *Earth Surface Dynamics*, *5*(4), 841–860. https://doi.org/10.5194/esurf-5-841-2017

Brooks, P. D., Chorover, J., Reinfelder, Y. F., Godsey, S. E., Maxwell, R. M., McNamara, J. P., & Tague, N. C. (2015). Hydrological partitioning in the critical zone: Recent advances and opportunities for developing transferrable understanding of water cycle dynamics. *Water Resources Research*, *51*(9), 6973–6987. https://doi.org/10.1002/2015WR017039

Chen, H., Niu, Q., McNamara, J. P., & Flores, A. N. (2023). Hydrologic modeling and field data for studying the role of subsurface critical zone structure on hydrological partitioning. [Dataset]. *HydroShare*. https://doi.org/10.4211/hs.d1537789fea8421aa3fe1cd2ec155b57

Chen, H., Niu, Q., Mendieta, A., Bradford, J., & McNamara, J. (2023). Geophysics-informed hydrologic modeling of a mountain headwater catchment for studying hydrological partitioning in the critical zone. *Water Resources Research*, *59*(12), e2023WR035280. https://doi.org/10.1029/2023WR035280

Dettinger, M., Udall, B., & Georgakakos, A. (2015). Western water and climate change. *Ecological Applications*, *25*(8), 2069–2093. https://doi.org/10.1890/15-0938.1

Dralle, D. N., Hahm, W. J., Rempe, D. M., Karst, N. J., Thompson, S. E., & Dietrich, W. E. (2018). Quantification of the seasonal hillslope water storage that does not drive streamflow. *Hydrological Processes*, *32*(13), 1978–1992. https://doi.org/10.1002/hyp.11627

Evans, S. G., Ge, S., & Liang, S. (2015). Analysis of groundwater flow in mountainous, headwater catchments with permafrost. *Water Resources Research*, *51*(12), 9564–9576. https://doi.org/10.1002/2015wr017732

Foster, L. M., Bearup, L. A., Molotch, N. P., Brooks, P. D., & Maxwell, R. M. (2016). Energy budget increases reduce mean streamflow more than snow–rain transitions: Using integrated modeling to isolate climate change impacts on Rocky Mountain hydrology. *Environmental Research Letters*, *11*(4), 044015. https://doi.org/10.1088/1748-9326/11/4/044015

Han, X., Liu, J., Srivastava, P., Mitra, S., & He, R. (2020). Effects of critical zone structure on patterns of flow connectivity induced by rainstorms in a steep forested catchment. *Journal of Hydrology*, *587*, 125032. https://doi.org/10.1016/j.jhydrol.2020.125032

Heidbüchel, I., Troch, P. A., Lyon, S. W., & Weiler, M. (2012). The master transit time distribution of variable flow systems. *Water Resources Research*, *48*(6). https://doi.org/10.1029/2011wr011293

Hughes, J. D., Russcher, M. J., Langevin, C. D., Morway, E. D., & McDonald, R. R. (2022). The MODFLOW Application Programming Interface for simulation control and software interoperability. *Environmental Modelling and Software*, *148*, 105257. https://doi.org/10.1016/j.envsoft.2021.105257

Kelleners, T. J., Chandler, D. G., McNamara, J. P., Gribb, M. M., & Seyfried, M. S. (2010). Modeling runoff generation in a small snow-dominated mountainous catchment. *Vadose Zone Journal*, *9*(3), 517–527. https://doi.org/10.2136/vzj2009.0033

Klos, P. Z., Lucas, R. G., & Conklin, M. H. (2023). Influence of critical zone architecture and snowpack on streamflow generation processes: A Mountain-Meadow headwater system in a Mediterranean climate. *Water Resources Research*, *59*(7), e2023WR034493. https://doi.org/10.1029/2023wr034493

Kormos, P. R., Marks, D., McNamara, J. P., Marshall, H. P., Winstral, A., & Flores, A. N. (2014). Snow distribution, melt and surface water inputs to the soil in the mountain rain–snow transition zone. *Journal of Hydrology*, *519*, 190–204. https://doi.org/10.1016/j.jhydrol.2014.06.051

Kormos, P. R., McNamara, J. P., Seyfried, M. S., Marshal, H. P., Marks, D., & Flores, A. N. (2015). Bedrock infiltration estimates from a catchment water storage-based modeling approach in the rain snow transition zone. *Journal of Hydrology*, *525*, 231–248. https://doi.org/10.1016/j.jhydrol.2015.03.032

Maxwell, R. M., & Kollet, S. J. (2008). Interdependence of groundwater dynamics and land-energy feedbacks under climate change. *Nature Geoscience*, *1*(10), 665–669. https://doi.org/10.1038/ngeo315

McDonnell, J. J., Spence, C., Karran, D. J., Van Meerveld, H. J., & Harman, C. J. (2021). Fill-and-spill: A process description of runoff generation at the scale of the beholder. *Water Resources Research*, *57*(5), e2020WR027514. https://doi.org/10.1029/2020wr027514

McNamara, J. P., Benner, S. G., Poulos, M. J., Pierce, J. L., Chandler, D. G., Kormos, P. R., et al. (2018). Form and function relationships revealed by long-term research in a semiarid mountain catchment. *Wiley Interdisciplinary Reviews: Water*, *5*(2), e1267. https://doi.org/10.1002/wat2.1267

Nielson, T., Bradford, J., Holbrook, W. S., & Seyfried, M. (2021). The effect of aspect and elevation on critical zone architecture in the Reynolds Creek critical zone observatory: A seismic refraction study. *Frontiers in Water*, *3*, 670524. https://doi.org/10.3389/frwa.2021.670524

Parsekian, A. D., Singha, K., Minsley, B. J., Holbrook, W. S., & Slater, L. (2015). Multiscale geophysical imaging of the critical zone. *Reviews of Geophysics*, *53*(1), 1–26. https://doi.org/10.1002/2014rg000465

Riebe, C. S., Hahm, W. J., & Brantley, S. L. (2017). Controls on deep critical zone architecture: A historical review and four testable hypotheses. *Earth Surface Processes and Landforms*, *42*(1), 128–156. https://doi.org/10.1002/esp.4052

Roa-García, M. C., Brown, S., Schreier, H., & Lavkulich, L. M. (2011). The role of land use and soils in regulating water flow in small headwater catchments of the Andes. *Water Resources Research*, *47*(5). https://doi.org/10.1029/2010wr009582

St. Clair, J., Moon, S., Holbrook, W. S., Perron, J. T., Riebe, C. S., Martel, S. J., et al. (2015). Geophysical imaging reveals topographic stress control of bedrock weathering. *Science*, *350*(6260), 534–538. https://doi.org/10.1126/science.aab2210

Wang, H., Tetzlaff, D., & Soulsby, C. (2018). Modelling the effects of land cover and climate change on soil water partitioning in a boreal headwater catchment. *Journal of Hydrology*, *558*, 520–531. https://doi.org/10.1016/j.jhydrol.2018.02.002

Welch, L. A., & Allen, D. M. (2012). Consistency of groundwater flow patterns in mountainous topography: Implications for valley bottom water replenishment and for defining groundwater flow boundaries. *Water Resources Research*, *48*(5). https://doi.org/10.1029/2011wr010901

White, A., Moravec, B., McIntosh, J., Olshansky, Y., Paras, B., Sanchez, R. A., et al. (2019). Distinct stores and the routing of water in the deep critical zone of a snow-dominated volcanic catchment. *Hydrology and Earth System Sciences*, *23*(11), 4661–4683. https://doi.org/10.5194/hess-23-4661-2019

Wlostowski, A. N., Molotch, N., Anderson, S. P., Brantley, S. L., Chorover, J., Dralle, D., et al. (2021). Signatures of hydrologic function across the critical zone observatory network. *Water Resources Research*, *57*(3), e2019WR026635. https://doi.org/10.1029/2019wr026635